# ELECTROCHEMICAL AND INFRARED STUDIES OF THE REDUCTION OF ORGANIC CARBONATES

Xuerong Zhang, Robert Kostecki, Thomas J. Richardson, James K. Pugh and Philip N. Ross, Jr.* Lawrence Berkeley National Laboratory, University of California Berkeley, California 94720

ABSTRACT

The reduction potentials of five organic carbonates commonly employed in lithium battery electrolytes, ethylene carbonate (EC), propylene carbonate (PC), diethyl carbonate (DEC), dimethyl carbonate (DMC) and vinylene carbonate (VC) were determined by cyclic voltammetry using inert (Au or glassy carbon) electrodes in THF/$LiClO_4$ supporting electrolyte. The reduction potentials for all five organic carbonates were above 1 V (vs. $Li/Li^+$). PC reduction was observed to have a significant kinetic hindrance. The measured reduction potentials for EC, DEC and PC were consistent with thermodynamic values calculated using density functional theory (DFT) assuming one-electron reduction to the radical anion. The experimental values for VC and DMC were, however, much more positive than the calculated values, which we attribute to different reaction pathways. The role of VC as an additive in a PC-based electrolyte was investigated using conventional constant-current cycling combined with ex-situ infrared spectroscopy and *insitu* atomic force microscopy (AFM). We confirmed stable cycling of a commercial lithium-ion battery carbon anode in a PC-based electrolyte with 5 mol % VC added. The preferential reduction of VC and the SEI layer formation therefrom appears to inhibit PC co-intercalation and subsequent graphite exfoliation.

---

* Corresponding author
email: PNRoss@lbl.gov
Fax: (510) 486-5530

## INTRODUCTION

Electrolytes typically used in lithium batteries consist of a lithium salt dissolved in an organic solvent, or a mixture of these solvents. The solvents fall into two general classes: ethers or alkyl esters of carbonic acid. Because of lower volatility and higher flash point, the organic carbonates are the preferred solvent class in commercial batteries. Propylene carbonate (PC) has many advantages over other organic carbonates for use in the battery electrolyte, e.g. lower cost and better low temperature performance. Use of PC in Li-ion batteries has, however, been problematic due to co-intercalation of solvent molecules along with $Li^+$ ion into the graphite and subsequent exfoliation [1]. The electrolyte commonly used in commercial lithium-ion cells is based on ethylene carbonate (EC), even though these batteries have poorer low temperature performance.[2] Research efforts have, with some success[3,4], pursued additives to PC to generate a SEI layer that prevents PC co-intercalation. The mechanism of functioning of these additives is, however, still uncertain.

We have performed quantum chemical calculations of the thermodynamic reduction potential of eleven organic molecules at an inert electrode assuming one-electron reduction.[5]. The ethers in general were found to be much more stable to reduction than the organic carbonates, and are not expected to be reduced before the deposition of lithium metal. The reduction potentials of organic carbonates were calculated to be positive to the lithium potential, with EC being the most positive, 1.46 V versus $Li/Li^+$. Here we report our experimental determinations of the reduction potentials of EC, PC, diethylcarbonate (DEC), dimethylcarbonate (DMC) and vinylene carbonate (VC), and compare them with calculated values. The postulated reduction reactions for the five organic carbonates discussed here are shown in the Scheme below. The role of

VC as an additive was also investigated and the SEI layer resulting from its reduction characterized by infrared spectroscopy.

## EXPERIMENTAL SECTION

Tetrahydrofuran (THF) (Aldrich, 99.9+%, HPLC grade), ethylene carbonate (EC) (Grant Chemical, less than 20 ppm $H_2O$), $LiClO_4$ (EM industries), DMC (Grant Chemical, less than 20 ppm $H_2O$), DEC (Grant Chemical, less than 20 ppm $H_2O$), PC (Grant Chemical, less than 20 ppm $H_2O$), and VC (Aldrich, 97%) were used as received without further purification. A single compartment glass cell with three electrodes was used for the electrochemical experiments. Lithium metal was used for both counter and reference electrodes. The target solvent specie was dissolved in a THF/0.1M $LiClO_4$ supporting electrolyte to a concentration typically of 1 vol % (5 mM in the case of EC). Three different working electrodes were used. A 1mm radius Au milli-electrode was used in cyclic voltammetry experiments. A glassy carbon electrode (1 cm x 1 cm) was used for the FTIR experiments with VC. A commercial (PolyStor, Inc, Pleasanton CA) Li-ion battery composite carbon electrode was used for the cycling. The composition of the anode was 75% MCMB carbon, 17% SFG-6 graphite, and 8% polyvinylidene difluoride (Kureha C) with a loading of 5.5 mg/cm$^2$ applied to both sides of a Cu foil current collector.

For the FTIR experiments, the glassy carbon electrode was cycled at 20 mV/s between 0.1 and 2 V, held at the VC reduction potential for five minutes, then brought back to 2 V. The electrode was emersed from the cell at 2 V, and inserted without rinsing into a gastight IR cell fitted with a KBr window. Ex-situ IR microscopy was conducted using a Nicolet Magna 760 spectrometer fitted with a Nic-Plan IR Microscope.

*In--situ* atomic force microscopy (AFM) images were obtained with a Molecular Imaging (MI) scanning probe microscope coupled with a Park Scientific Instruments (PSI) electronic controller. The electrochemical cell is composed of three electrodes, with glassy carbon being the working electrode and lithium foil being the reference and counter electrode. The AFM was used in the constant-force mode with PSI MLCT-AUNM microcantilevers (0.05 $Nm^{-1}$) to determine the morphology of the carbon electrode surface. These measurements were conducted in a small glove-box under helium atmosphere.

RESULTS AND DISCUSSION:

Electrochemical Studies

Solvent reduction potentials were determined by cyclic voltammetry (CV). The sweep rates were 2 – 5 mV/s. The solvent specie was dissolved in a THF/$LiClO_4$ supporting electrolyte to a concentration of ca. 1 vol %. A low concentration was used to minimize the effect of impurities, e.g. water and the inhibitor in VC, on the Voltammetry. THF was selected because of its stability towards reduction above the lithium metal potential, as seen from the "control" scans (Figure 1). The cathodic peak at 1.8 V is generally ascribed to the reduction of $H_2O$ or oxygen impurities in the electrolyte[6]. The coupled peaks at around 0.6 V (cathodic) and 0.9 V (anodic) correspond to underpotential deposition (UPD) and anodic stripping, respectively, of lithium metal on the gold surface. The UPD of Li from ethereal solvent is more complex than for other metals in aqueous electrolyte, as discussed at length by Aurbach et al[6].

Characteristic voltammetry curves for the organic carbonates are shown in Figure 1 and the reduction potentials are summarized in Table 1. The experimental values for EC, DEC, and PC are in reasonable agreement with the calculated values, while those for

DMC and VC are significantly lower. For EC and PC, the calculation assumes one-electron transfer to form the bond broken form of radical anion (see Scheme 1 and 2). The reduction of the two linear carbonate solvents (DEC and DMC) was assumed[5] to have another one-electron-transfer to the alkyl radical that was broken off from the radical anion generated initially, and formed a alkyl anion. The first electron transfer breaks the C-O bond forming an alkyl carbonate anion and an alkyl radical, and the 2nd electron transfer is to the alkyl radical to form an alkyl anion (see Scheme). The reduction potential calculated based on this assumption is in good agreement with the experimental values for DEC, but not for DMC. It is energetically unfavorable for a methyl radical to accept an electron to form a methyl anion, which consequently lowers the calculated reduction potential for DMC versus that for DEC. This implies that the reduction of DMC follows a different reaction pathway. The reduction potential of VC was calculated with 5A rather than 5B being the final product due to instability of the vinyl radical in 5B. The high experimental reduction potential obtained for VC implies a different reaction pathway for this molecule as well.

EC was the only solvent that produced a single reduction peak on the first cathodic sweep, the others having some ill-defined cathodic process(es) below 0.5 V. The product formed by the initial reduction of EC appears to be more stable than that formed by reduction of the other carbonates. It is also the only carbonate in which Li UPD is clearly seen, as in the supporting THF electrolyte, indicating the reduction product of EC does form a functioning SEI layer on Au. This chemistry is consistent with the general acceptance of EC-based electrolyte in lithium-ion batteries.

The CV of PC reduction has (not shown) a shallow and broad feature ranging from 1.6 to 1 V, most probably indicating slow reduction kinetics. This is consistent with most of the literature reports on PC reduction. Aurbach et al. also did not observe a

clearly resolved feature for PC reduction on Au, only a large cathodic background current that was ascribed to the solvent reduction[6]. While a definite reduction potential could not be established, their concurrent FTIR results indicated that PC reduction occurred at a potential as high as 1.5 V. Campbell[7] reported a similar result in neat PC with a Pt microelectrode, a broad cathodic wave beginning at 1 V. The use of neat solvent eliminated the possibility of salt reduction, and the cathodic process beginning at ca. 1 V was assigned to the reduction of PC. The same group also reported the presence of water or 1,2-propanediol in PC enhanced the cathodic current. Pletcher et al. [8] observed simliar cathodic current in PC based electrolyte with a Ni electrode. They argued, however, that the observed magnitude of the cathodic current was too small for solvent reduction at such a high concentration of PC and therefore, could not be ascribed to its reduction. They proposed that it was more likely the reduction of trace water. The PC concentration in the THF supporting electrolyte in our experiments was 1 vol %. The amount of water introduced by PC addition, therefore, would be very small. The observed reduction in electrolyte with PC, which was not seen in the supporting THF electrolyte, should indeed be reduction of the PC solvent. The slow kinetic makes it impossible to assign a definite value to the reduction potential, it lies somewhere in the range of 1 – 1.6 V. The calculated value of 1.24 V is within this range. PC's slow reduction kinetics is consistent with the general understanding that PC is co-intercalated first with $Li^+$ into graphite electrode and subsequently reduced inside, which causes exfoliation of the electrode.

The relatively positive reduction potential for VC supports one of the postulated mechanisms of action of VC as an additive to PC-based electrolyte for Li-ion cells. Similar to EC, preferential reduction of VC could form an interfacial layer that prevents PC co-intercalation and graphite exfoliation.

<u>The Effect of VC as Additive in PC electrolyte:</u>

Figure 2a shows constant-current (0.5 mA/cm$^2$) cycling of the composite carbon anode in PC electrolyte with 1 M $LiClO_4$. The long plateau around 0.4 V indicates significant solvent reduction. In consequence, the reversible capacity for the first cycle was only 12%. Severe graphite exfoliation was observed in this electrolyte after just 10 cycles, and concurrent loss of capacity. Figure 2b shows the first constant-current charge and discharge of a nominally identical composite carbon anode in the same PC with addition of 5 vol% VC. The reversible capacity on the first cycle is significantly improved to 67%, and subsequent cycles had a cycling efficiency of 93 – 95 %. The electrolyte turned slightly brown after 10 cycles. There was, however, no observable exfoliation of the graphite. The effects of VC on PC reduction reported here are qualitatively consistent with those reported previously by Jehoulet et al. [4]. This group focussed on gas production during the formation charge, and demonstrated that the amount of gas produced in a PC/EC/DMC mixed solvent decreased significantly when 5% VC was added. This was attributed to a suppression of solvent decomposition. The same group also reported that the electrochemical reduction of VC did not release gaseous product.

VC is reduced at 1.40 V, much higher than the calculated value of 0.25 V, which suggests that one-electron transfer does not stop at the unsaturated radical anion (5A in Scheme) as was assumed in the calculation [5]. Rather, a more energetically favorable intermediate is formed. Infrared reflection absorption (IRRAS) spectroscopy was used to investigate the chemistry of VC reduction. The results (Figure 3) indicate that VC molecule is reduced to unsaturated alkylcarbonate anion. IRRAS spectra from the surface of the glassy carbon electrode held at 1.2 V in THF supporting electrolyte with 5 vol% VC shows new peaks different from the supporting electrolyte, and attributed to VC reduction. The absorption peak at 1640 cm$^{-1}$ corresponds to the C=O stretching mode of

an alkyl carbonate, and 1620 $cm^{-1}$ is assigned to the C=C double bond stretching mode. Note that the C=C double bond stretch is missing in the spectrum of the electrolyte before reduction due to the symmetry of the VC molecule, i.e. there is zero dipole moment. Its appearance in the IR spectra after reduction suggests a ring opening of VC, which creates an unsymmetrical environment about the C=C bond, and causes it to be IR-active. The broad shoulder at 980 $cm^{-1}$ is assigned to the out-of-plane C-H bending mode of a methylene ($=CH_2$) group [9]. All of these point to lithium vinyl carbonate as one of the reduction products of VC, and a major component in the organic layer of the SEI. The suggested reduction mechanism of VC reduction, shown in the Scheme, involves the formation of a bond-broken radical anion (5B), which undergoes a hydrogen abstraction to produce the unsaturated alkylcarbonate anion (5C). The spectrum for the bulk electrolyte after reduction shows similar features to that from the electrode, which suggests that the lithium vinyl carbonate salt is partly soluble in the electrolyte.

IRRAS spectra were also obtained from the composite carbon electrode cycled in PC electrolyte with and without the 5 % VC additive (not shown). Although the quality of the spectrum from this porous electrode was not equal to those from the glassy carbon, the IR features assigned to VC reduction products were observed. This suggests that VC reduction takes place at potentials above 1.2 V, before $Li^+$ ion intercalation, and forms a protective layer that prevents PC co-intercalation and graphite exfoliation. Although the other carbonates EC, DEC and DMC also have reduction potentials positive of $Li^+$ ion intercalation, use of EC/DEC/DMC as *additives* to PC, i.e. at the concentrations of a few vol %, does not produce the same protection against graphite exfoliation as VC. The difference would appear to be due to the unique morphology and/or microstructure of the reduction layer formed by VC reduction.

*In-situ* AFM measurements were carried out to investigate the electrode surface morphology during the electrochemical reduction of the 1% VC in THF, 0.1 $LiClO_4$ electrolyte at a glassy carbon electrode. Figure 4A shows a typical image of a freshly prepared glassy carbon electrode held at open circuit potential (OCP) c.a. 2.0 V. The image displays a fairly uniform carbon surface with the average roughness of ~ 3.27 nm. The randomly scattered shallow scratches and point defects on the surface were produced during the polishing process.

The electrode potential was gradually decreased at 100 mV intervals from the initial OCP (2.0 V) to 0.8 V. A series of AFM images were recorded at each potential step. The AFM pictures were analyzed to find a correlation between the surface morphology and the CV characteristic. Visual examination of the AFM images reveals the presence of a surface film at 1.2 V (Figure 4 B), which becomes fully formed at 0.8 V (Figure 4 C). The film consists of tightly packed grains of ~50 nm distributed uniformly over most of the surface except for a few deeper scratch marks.

To determine the thickness of the surface film after polarization at 0.8 V, we used the experimental procedure which was previously applied to the SEI films on HOPG[10]. A 1 x 1 μm area of the electrode surface was selected and the SEI film was removed by abrasive etching i.e. repeated scanning of the AFM tip at high tip-to-sample force till no change of the surface morphology could be further induced. Following the abrasive etching, the electrode surface was scanned over a larger 5 x 5 μm area to image a cavity created in the SEI layer. Figure 5 shows the electrode morphology image with a square cavity in the center of the image and the corresponding height profile across the modified area. The AFM experiments were carried out at OCP at the end of multiple potential-step descent from 2.0 to 0.8 V. The thickness of the SEI film determined from the height profile was estimated C.A. 120 Å. However, it cannot be excluded that during prolonged

(~2min) polarization at constant potential the film grew thicker, especially at lower potentials, than during a single cathodic voltammetric scan. The voltammetric scans which are shown in Fig. 1 were recorded at 2-5 mV/s rate which is ~2-3 times faster than the potentiostatic experiment combined with the AFM imaging..

To provide more insight into SEI film formation, a statistical analysis of the AFM images was conducted. Average roughness of a 2 x 2 μm area from the same location at the electrode surface was calculated and expressed as a function of electrode potential (Figure 6). The electrode roughness decreased from 3.25 to 3.08 nm at potentials from 1.8 V to 1.5 V and then increased slightly at potentials lower between 1.4 and 1.2 V. Further decrease of potential combined with prolonged polarization produced substantial changes in electrode morphology and led to a significant increase of surface roughness to reach 3.65 nm (at 0.8 V). The initial drop of surface roughness at potentials below 1.8 V is consistent with formation of a thin featureless film which predominantly fills small cavities and scratches on the surface, i.e. smoothening it out. This layer could be a result of precipitation of LiOH, a product from the water reduction which starts at 1.8 V. As the reduction of VC takes place at 1.4 V ($2^{nd}$ reduction wave, see Figure 6), a surface layer with different morphology begins to develop. As a result, the electrode surface average roughness increases significantly. This is consistent with the formation of lithium vinyl carbonate salt observed by IRRS discussed earlier in the paper.

## SUMMARY

The electrochemical reduction of five organic carbonates, EC, PC, DEC, DMC and VC were studied via cyclic voltammetry at a Au electrode. More detailed studies of the chemistry of VC reduction were carried out using IRRAS at a glassy carbon electrode. The measured reduction potentials for EC, DEC and PC were consistent with thermodynamic values calculated using density functional theory (DFT) assuming one-

electron reduction to the radical anion. The experimental values for VC and DMC were, however, much more positive than the calculated values, which we attribute to different reaction pathways. The role of VC as an additive in a PC-based electrolyte was investigated. We confirmed stable cycling of a commercial lithium-ion battery carbon anode in a PC-based electrolyte with 5 mol % VC added. A surface layer indicative of preferential reduction of VC in the PC-based electrolyte was observed by IRRAS. The in-situ electrochemical AFM study provided a clear evidence of the SEI layer formation on the glassy carbon electrode in the 1% VC in THF, 0.1 $LiClO_4$ electrolyte when the potential was stepped down to 0.8 V. The preferential reduction of VC and the SEI layer formation therefrom appears to inhibit PC co-intercalation and subsequent graphite exfoliation.

ACKNOWLEDGEMENTS

This research was funded by the Assistant Secretary for Energy Efficiency and Renewable Energy, Office of Advanced Automotive Technologies, U. S. Department of Energy, under contract DE-AC03-76SF00098.

List of Figures

REFERENCES

(1) Besenhard, J. O.; Fritz, H. P. *J. Electrochem. Soc.*, **53**, 329 (1974).

(2) Winter, M.; Besenhard, J. O.; Spahr, M. E.; Novak, P. *Adv. Mater.*, **10**, 725 (1998).

(3) Wang, C.; Nakamura, H.; Komatsu, H.; Yoshio, M.; Yoshitake, H. *J. Power Sources*, **74**, 142 (1998).

(4) Jehoulet, C.; Biensan, P.; Bodet, J. M.; Broussely, M.; Moteau, C.; Tessier-Lescourret, C. *ECS Meeting Abtracts*, *vol. MA 97-2*, 135 (1997).

(5) Zhang, X.; Pugh, J. K.; Ross, P. N. submitted to The Electrochemical Society Proceedings Series, Pennington, NJ (2000).

(6) Aurbach, D.; Daroux, M.; Faguy, P.; Yeager, E. *J. Electroanal. Chem*., **297**, 225 (1991).

(7) Campbell, S. A.; Bowes, C.; McMillan, R. S. *J. ELectroanal. Chem.,* **284**, 195 (1990).

(8) Pletcher, D.; Rohan, J. F.; Ritchie, A. G. *Electrochim. Acta*; **39**, 1369 (1994).

(9) Smith, B. *Infrared spectral interpretation*; CRC Press LLC:, (1998).

(10) Alliata, D.; Kötz, R.; Novák, P.; Siegenthaler, H. *Electrochem. Commun*. In press.

Table 1. Comparison of calculated[5] and experimental potential values of solvent reduction.

| Solvent | Calculated | Experimental |
|---|---|---|
| EC | 1.46 | 1.36 |
| DEC | 1.33 | 1.32 |
| PC | 1.24 | 1.00 – 1.60 |
| DMC | 0.86 | 1.32 |
| VC | 0.25 | 1.40 |

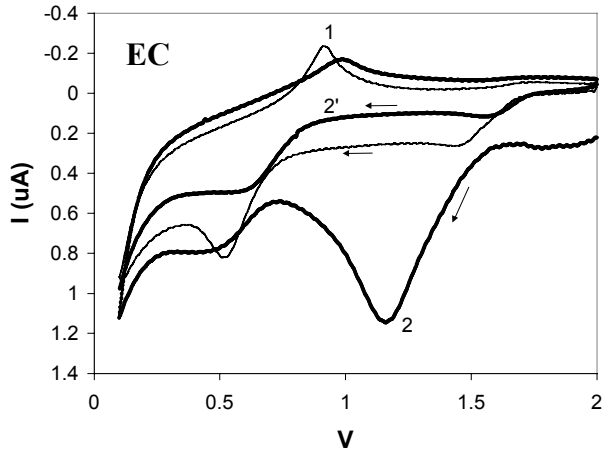
EC
1
2'
2
I (uA)
V
-0.4
-0.2
0
0.2
0.4
0.6
0.8
1
1.2
1.4
0
0.5
1
1.5
2

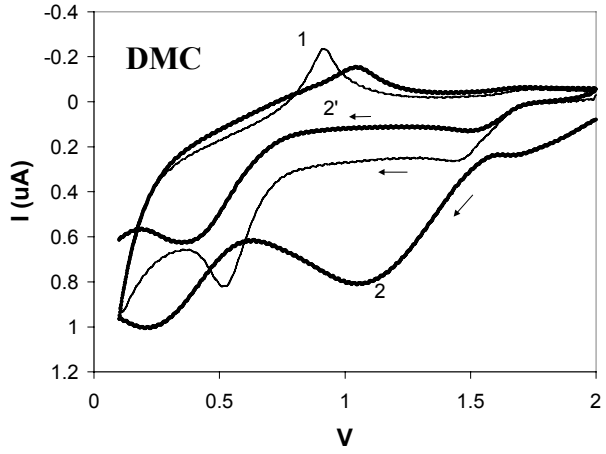
DMC
1
2'
2
I (uA)
V
-0.4
-0.2
0
0.2
0.4
0.6
0.8
1
1.2
0
0.5
1
1.5
2

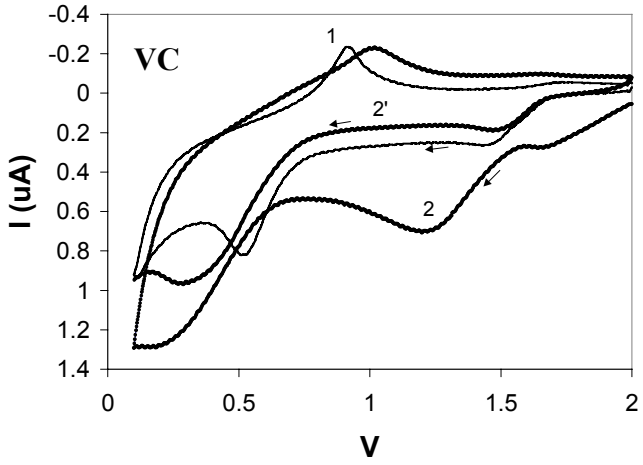
VC
1
2'
2
I (uA)
V
-0.4
-0.2
0
0.2
0.4
0.6
0.8
1
1.2
1.4
0
0.5
1
1.5
2

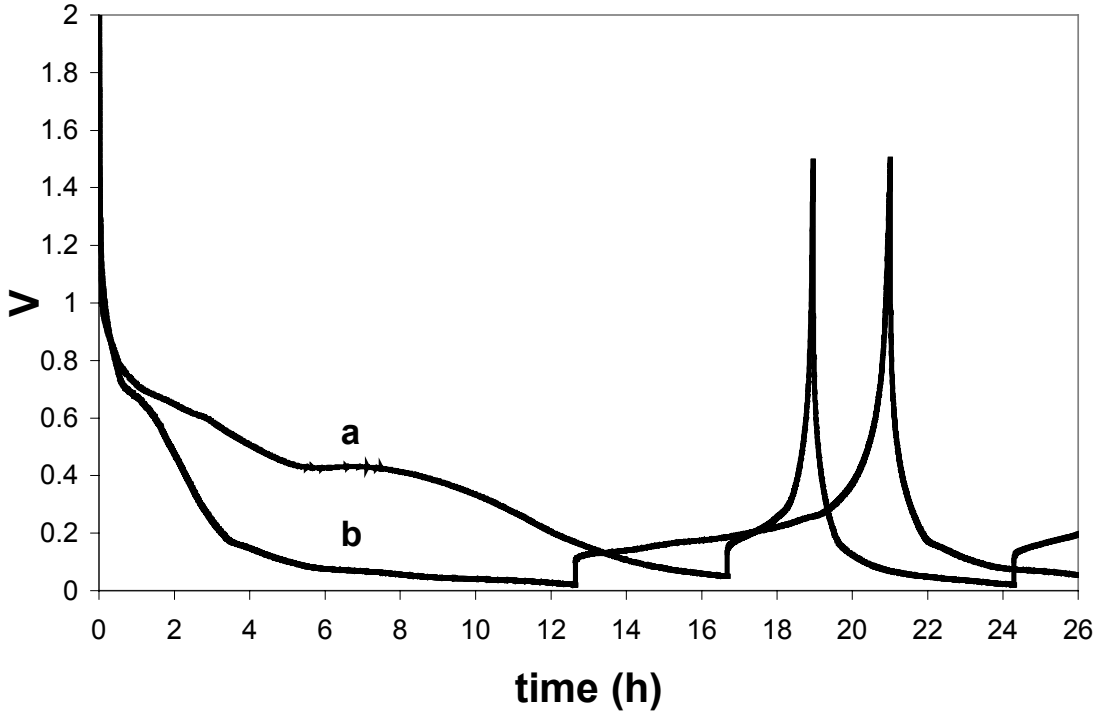
2
1.8
1.6
1.4
1.2
1
0.8
0.6
0.4
0.2
0
V
a
b
0
2
4
6
8
10
12
14
16
18
20
22
24
26
time (h)

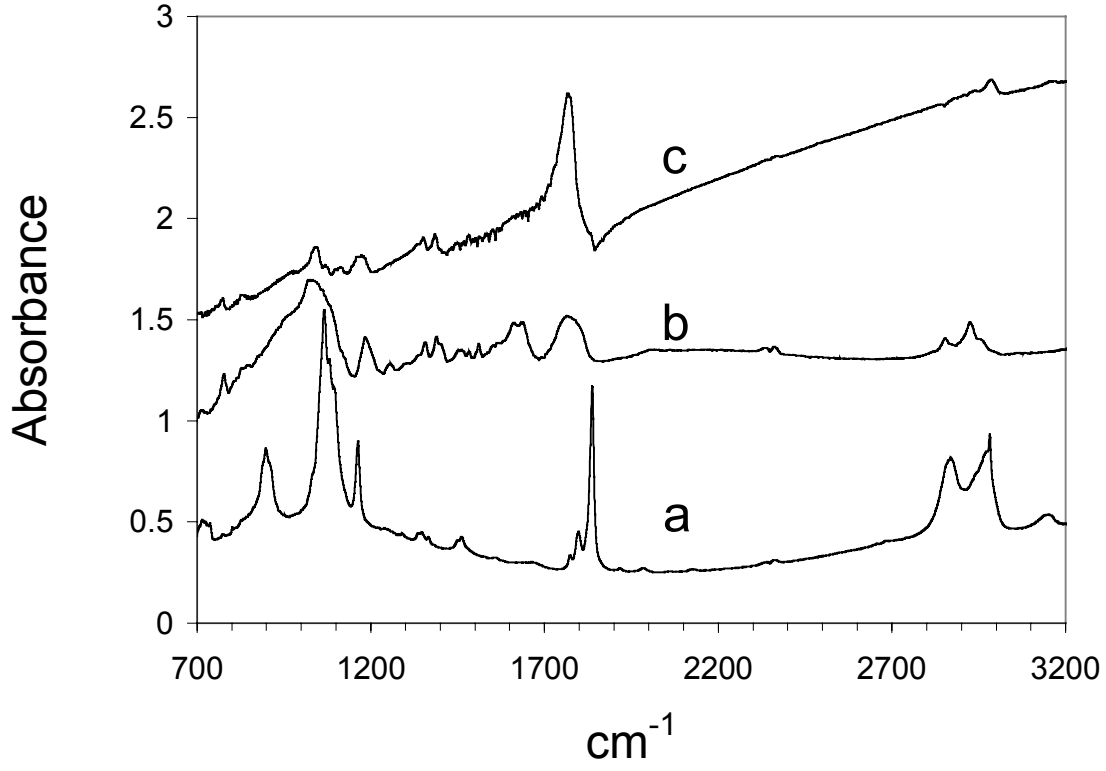
Absorbance
3
2.5
2
1.5
1
0.5
0
c
b
a
700
1200
1700
2200
2700
3200
cm-1

**(A)**

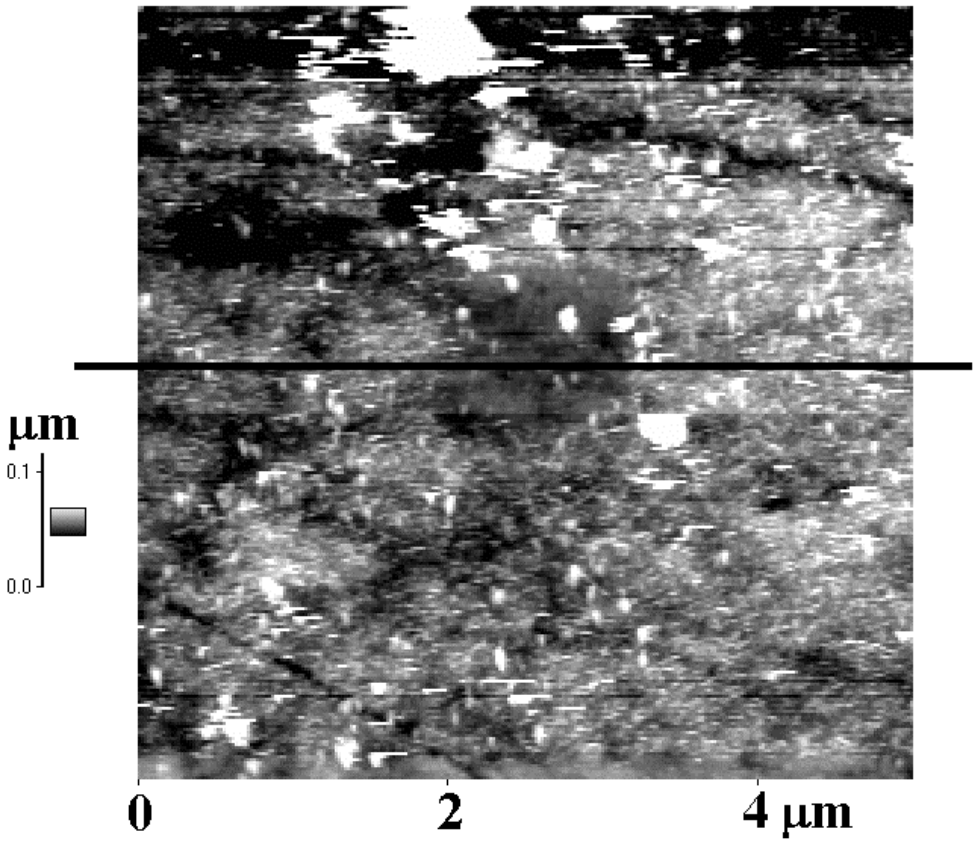


**(B)**

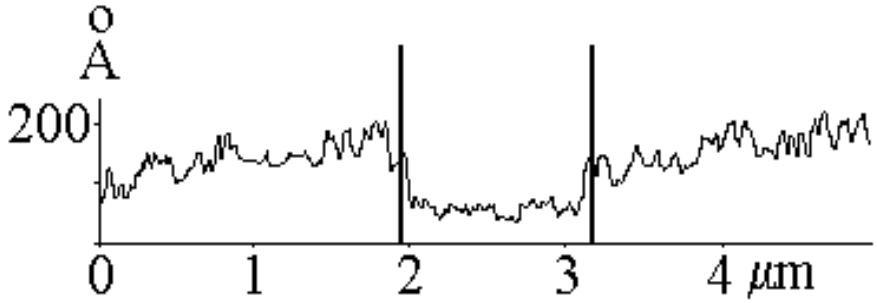

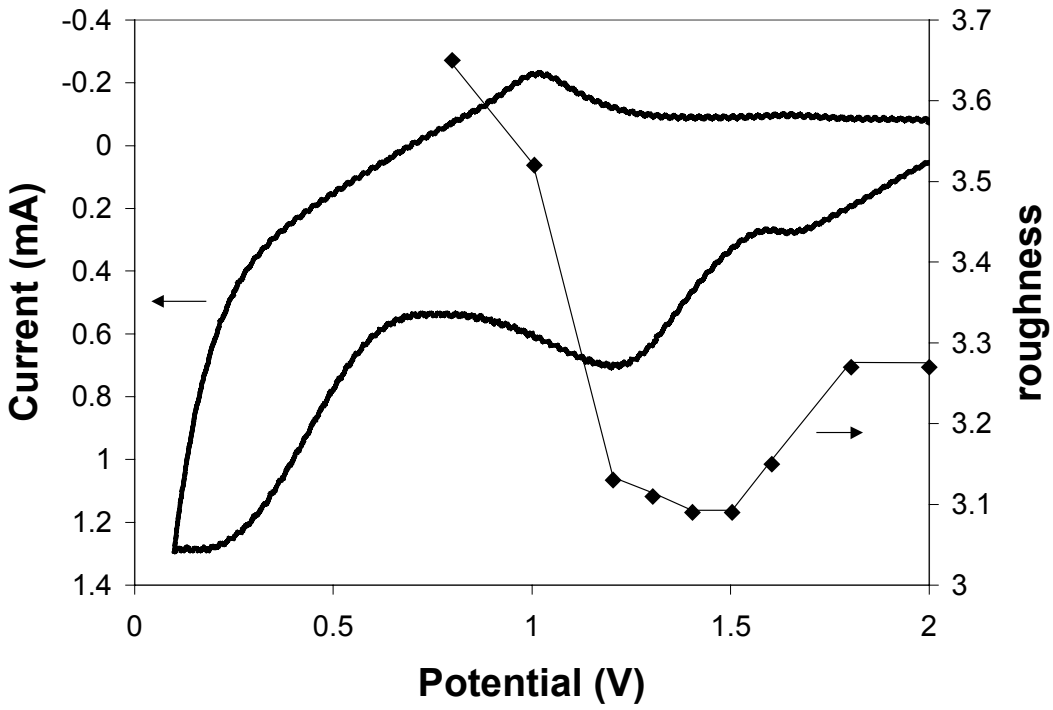
-0.4
-0.2
0
0.2
0.4
0.6
0.8
1
1.2
1.4
Current (mA)
3.7
3.6
3.5
3.4
3.3
3.2
3.1
3
roughness
0
0.5
1
1.5
2
Potential (V)